JOURNAL OF APPLIED ELECTROCHEMISTRY 12 (1982) 669–680

Studies of the kinetics of the lithium/aluminium electrode in molten LiCl–KCl by linear sweep voltammetry

Y. S. FUNG

University of Hong Kong, Pokfulam Road, Hong Kong

D. INMAN

Department of Metallurgy, Imperial College, London, UK

S. H. WHITE

EIC Laboratories Inc., 55 Chapel Street, Newton, Massachusetts 02158 USA

Received 1 February 1982

The deposition of lithium on aluminium leads initially to the formation of a solid solution, followed by the precipitation of various lithium/aluminium alloys. Several fundamental phenomena such as monolayer formation and nucleation were shown to affect the kinetics of the deposition process. In the present investigation, the cyclic voltammetric technique (fast) was used to study these phenomena. It is a very useful technique for the qualitative understanding of the deposition process and in its scanning coulometric modification, which is also utilised in this investigation, it can provide useful semi-quantitative information.

Voltammetric profiles corresponding to the formation of the α-phase (a solid solution of Li and Al), the β-phase (LiAl) and the γ-phase (Li_3Al) amongst others, were identified and their characteristics investigated. The results are discussed against the background of the possible vitiating effects of impurities in the present paper.

1. Introduction

The well tested lithium/aluminium electrode has so far proved to be the most promising anode for use in the high-temperature molten salt lithium/iron sulphide battery [1, 2]. The retention of lithium is good and the potential is stable throughout the α/β phase transformation from 9 at % to 50 at % lithium [3]. However, only very few fundamental studies of the kinetics of the electrode have been carried out and these have concentrated for the most part on the β-phase [4–7].

The deposition of lithium on aluminium occurs with extensive alloy formation. Several fundamental phenomena seem to affect the kinetics of the deposition process, viz. undervoltage deposition, monolayer formation, nucleation polarization and the formation of successive alloys with increasing lithium contents.

The present study is concerned with the light that linear sweep voltametry throws on these phenomena, particularly in the case of the deposition (i.e., charging) process. The aim has been to complement those studies which have already been carried out using different electrochemical as well as structural techniques. Particular attention has been paid to the processes which occur during overcharge and overdischarge conditions, that is well away from the usual range of operation of the cell but nevertheless conditions which could easily be encountered in the battery situation.

Although the rapid linear sweep voltammetric technique is a very powerful one for unravelling the complexities of multistep electrode processes [8–12], it does have some disadvantages in the present case because of the changes of electrode geometry which occur during charging and discharging. Because of this, linear sweep voltammetry can best be regarded as a semi-quantitative tool in the present context. Nevertheless its

0021–891X/82/060669–12$03.94/0

usefulness lies in its ability to scan the whole potential range and to provide in effect an "electrochemical spectrum". The useful potential range extends from + 1.2 V to − 0.7 V vs a β-phase Li/Al reference electrode (see below). $AlCl_3$ is evolved at the anodic limit and alkali metals are deposited in massive quantities at the cathodic limit. Two types of peak are present in the 'electrochemical spectrum': intrinsic peaks which arise from the deposition and stripping of alkali metals from various solid solutions and alloys and extrinsic peaks which, in spite of rigorous purification, can arise from the oxidation and reduction of various oxides, hydroxides and water. Moreover, useful information can also be obtained by varying the scan rate as well as the scan range. As a matter of fact, the formation of the γ-phase and other lithium-rich intermetallic phases can only be studied using a fast sweep rate so as to avoid exceeding the current limit of the potentiostat. Furthermore, some semi-quantitative information can also be obtained using a scanning coulometric modification [13–15].

2. Experimental procedure

2.1. *Electrolyte and electrodes preparation*

The purification of the LiCl–KCl eutectic used as the solvent and the procedure for the assembly of the reaction cells have been described elsewhere [16]. In any event, molten salt methodology is now becoming increasingly well known and several general texts describing it are available or will shortly become available [17]. Ag/AgCl (0.2 mol %) was used as the reference electrode, along with Li/Al alloyed in the β-phase, particularly in later experiments. The reasons are that the Li/Al reference electrode is much easier to prepare and can be formed *in situ* immediately before the experiment in a few minutes. Moreover, its potential is always close to the working electrode potential during cycling [− 2.27 V vs the Ag/AgCl (0.2 mol %) electrode]. Thus, it is much simpler for recording as no external offset voltage is required for using the Li/Al as the reference electrode (see the apparatus section). In early experiments, a graphite electrode was used as the counter electrode but as the chlorine liberated was found to be detrimental to the other cell components, a thermally preformed Li/Al electrode was used as the counter electrode in later experiments. The working electrode was an aluminium wire, diameter 0.74 mm, supplied by BDH. A typical set-up for the experimental cell is shown in Fig. 1. The thermally formed counter electrode was precleaned to remove the Li/Al particles breaking away from the electrode due to thermal expansion during heating overnight in a separate glass chamber under the LiCl/KCl eutectic immediately before each experiment. It was then pushed up and twisted in such a way that is was clear of the cleaning chamber before being reimmersed in the melt for use as shown in Fig. 1. The arrows indicate the sequence of movements. The glass chamber was then removed from the melt to avoid a corrosion effect with the Li/Al alloy. All the electrodes and the purified melt were assembled inside a dry box and the experiment was carried out in the cell under a slight positive pressure of argon.

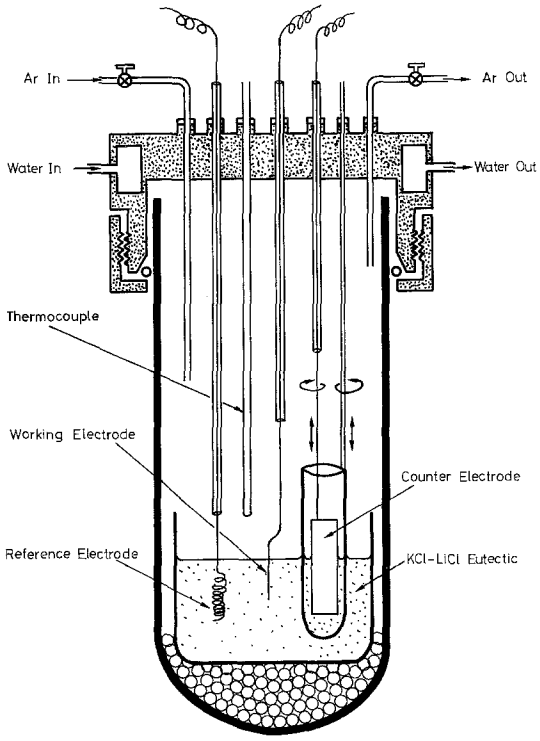

Fig. 1. Schematic diagram of a typical set-up for the experimental cell. This figure was originally presented at the Fall 1980 Meeting of the Electochemical Society, Inc. held in Hollywood, Florida, USA.

2.2. *Apparatus*

The electrode potentials were controlled using a Wenking Potentiostat Control Amplifier 72L. As the maximum offset voltage is 1 V, an external offset voltage is required when using the Ag/AgCl (0.2 mol %) reference electrode at the rest potential, whereas the Li/Al electrode requires no such complication. The current output was recorded using a Bryans 26000 X–Y recorder. In the case of very fast signals, they were recorded by a Datalab DL 501 transient recorder with a Tektronix 564 oscilloscope attachment for temporary viewing. They were later reproduced at a slower rate on the Bryans X–Y recorder. Four methods were used to measure the charge passed to the electrode in the scanning coulometry experiment. The initial two manual methods were quickly superseded by two electronic methods. (a) A Bentham Hi-Tek integrator was used to measure the charge directly. This is a very convenient method to measure the charge passed between the rest potential and the switching potential, as the instrument can be operated either on the total charge passed or on the positive charge alone. However, it cannot be used to measure the charge passed at intermediate potentials. (b) An electronic integrator, built in this laboratory, was used to measure the charge passed from the rest potential to the switching potential. The integration can be initiated, held or terminated by an external TTL trigger or manually and the initial potential can be set to a potential other than zero. The design is such that if the initial potential is set to a potential other than zero, the charges in the anodic as well as the cathodic sweep can be measured.

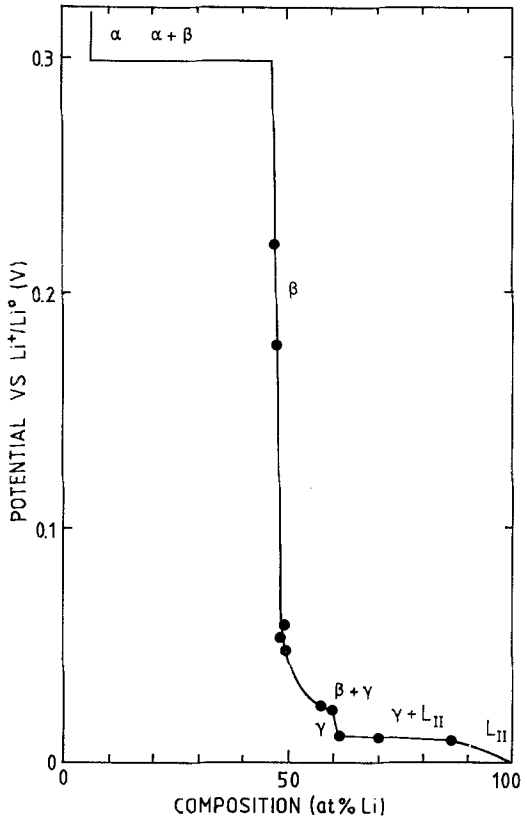

Fig. 2. EMF – composition diagram of lithium–aluminium alloy at 700 K. This figure was originally presented at the Fall 1980 Meeting of the Electrochemical Society, Inc. held in Hollywood, Florida, USA.

3. Results and discussion

3.1. *General aspects*

As a framework for discussing the voltammetric behaviour of the electrode, the plot of electrode potential vs composition from the paper by Selman *et al.* [3], (Fig. 2), is very useful. This shows clearly the intervals of stability of the various solid solutions and intermetallic compounds for the Li/Al system *at equilibrium.* The battery is usually operated in the 9 at % to 50 at % two phase transition region so that the cell potential will be constant during discharging. In order to avoid the formation of any lithium/aluminium alloy and to prevent the evolution of aluminium chloride before the experiment, the aluminium working electrode was always held at a potential of about + 0.7 V (vs the LiAl reference electrode) to protect it cathodically before applying the voltammetric sweeps.

3.2. *Cathodic to anodic switching potential in the α-phase (solid solution) region*

Figure 3 shows a typical cyclic voltammogram corresponding to the region where the deposited lithium forms a solid solution (the α-phase) [18–20] with the substrate aluminium. Lithium begins to deposit in fact at + 0.4 V vs the Li/Al reference electrode but it is noteworthy that there is no corresponding anodic stripping peak (it should be noted of course that there is no

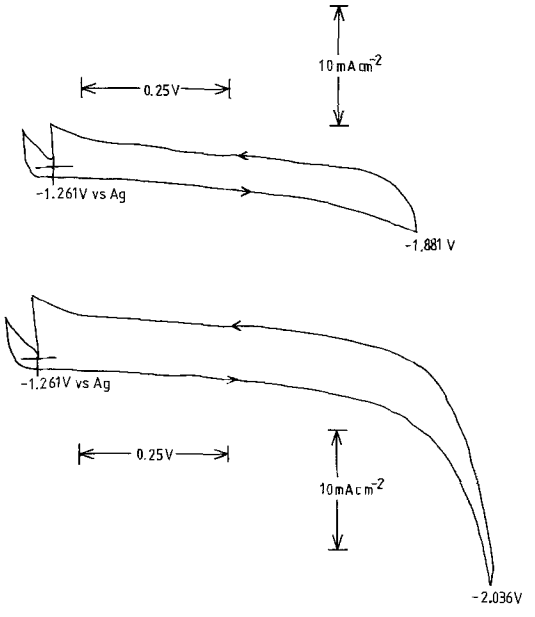

Fig. 3. The formation of the α-phase on the aluminium electrode. Sweep rate; 100 mVs^{-1}. This figure was originally presented at the Fall 1980 meeting of the Electrochemical Society, Inc. held in Hollywood, Florida, USA.

cathodic peak anyway). Coulombic efficiency is low and, especially at the cathodic end, the current is much smaller at the same potential during the reverse scan than during the forward scan. Since the sizes of the lithium and aluminium atoms are similar (0.155 nm and 0.138 nm respectively) transportation of the lithium within the aluminium will probably be by a vacancy mechanism. The voltammetric behaviour is typical of that for the formation of a solid solution, i.e., the final equilibrium sites of the lithium atoms have a range of energies and therefore the solid solution does not form at a discrete (sharply defined) electrode potential. Moreoever, at the onset of the deposition, there are plenty of active sites present. Their number will be reduced as more lithium is deposited so there is subsequently a tendency for the current to be lower at the same potential during the reverse sweep. Furthermore, as the potential goes more negative, less energetic sites at the electrode surface will be used up in the deposition process. Thus, there exists an energy distribution for all the lithium deposited and this can give rise to the absence of a stripping peak on the reverse sweep. Also, it is difficult to remove the lithium atoms after deposition because of their low rates of diffusion in the solid solution [21, 22]. Both of the above reasons explain the apparent lack of a 100% coulombic efficiency during the potential sweep, though the impurities present in the solution may also be another contributing factor.

3.3. *Switching potential in the β-phase formation region*

Figure 4 shows what happens when the switching potential is shifted in the cathodic direction and beyond what is obviously a critical value. The much larger currents which flow at the cathodic end are marked by sharp anodic stripping peaks. This phenomenon can be related to the formation and stripping of the β-phase (the compound Li/Al) which has a much more open structure than the α-phase (bcc, a = 0.637 nm compared with the fcc structure a = 0.405 nm of the α-phase, which is in effect an expanded Al lattice) [18–20, 23] and occurs over a narrow range of electrode potentials. It is also interesting to see that the current is much bigger on the reverse sweep at the same potential once the β phase is formed. The appearance of the more open β phase on the α phase at the electrode surface will certainly change the surface properties, decreasing the surface energy and enhancing the deposition of lithium. Moreover, the dissolution of lithium from the lattice of the β phase will create new frozen vacancy sites for lithium deposition, as the surface will take time to reorganize back to the aluminium lattice. Thus, the current will increase in the reverse sweep at the same potential compared with the forward sweep. The sharp peak and the existence of a critical potential for the formation of the β phase indicates that the β phase is more homogeneous in its energy distribution. As the potential shifts in a more cathodic direction the current corresponding to the formation and the stripping of the β phase will eventually outweigh those due to the α phase and the voltammogram will appear mainly due to the formation of the β phase (Fig. 4).

3.4. *The effect of repetitive cycling*

This is exemplified in Fig. 5 which shows the increases of current which occur in both the

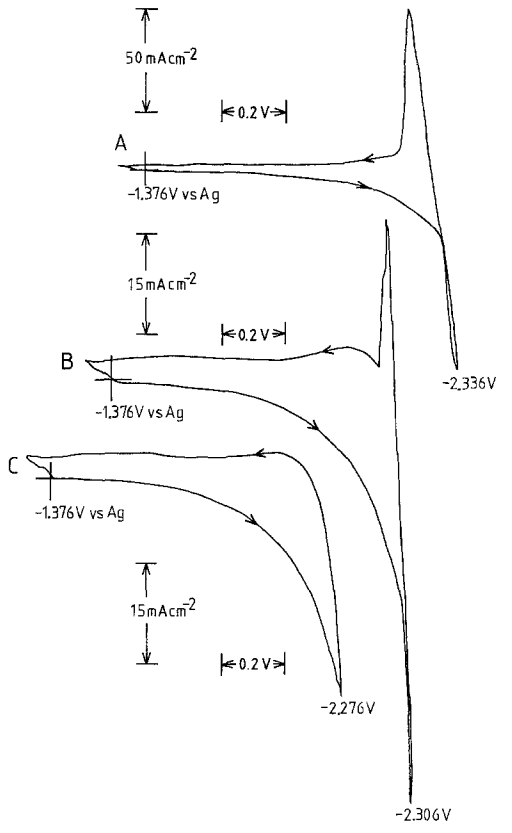

Fig. 4. The formation of the β-phase on the aluminium electrode. Sweep rate: 100 mVs^{-1}. This figure was originally presented at the Fall 1980 meeting of the Electrochemical Society, Inc. held in Hollywood, Florida, USA.

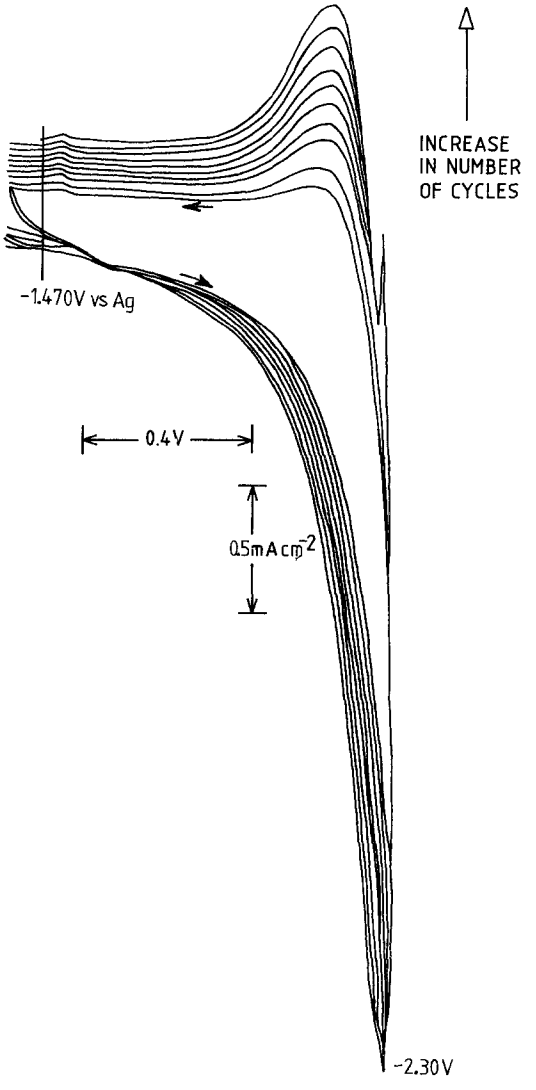

Fig. 5. The effect of cycling on the deposition and stripping of lithium from aluminium. Sweep rate: 100 mVs^{-1}. This figure was originally presented at the Fall 1980 meeting of the Electrochemical Society, Inc. held in Hollywood, Florida, USA.

cathodic and anodic modes during repetitive cycling. This phenomenon is known as the development of the electrode and arises from two factors (a) an increase of the surface area of the electrode due to a roughening effect and (b) the creation of new frozen vacancy sites for the accommodation of deposited lithium atoms by the selective *dissolution* of lithium during the anodic cycles.

3.5. *The behaviour of newly-immersed aluminium electrodes*

The importance of surface properties is also exemplified by the cyclic voltammetric behaviour of a new-immersed aluminium electrode, shown in Fig. 6. New, very sharp, cathodic and anodic waves can be seen at + 0.63 V and + 0.75 V respectively, vs the Li/Al reference electrode. The sharpness of the peaks indicates that they may originate from adsorption phenomena. As the charge under one of these peaks is roughly 200 μC cm^{-2} and that for the formation of a monolayer [24, 25] of lithium about 250 μC cm^{-2}, it is tempting to speculate that they arise from the formation and stripping of the latter. However, as indicated by Fig. 7, the repeated deposition and dissolution of lithium over the α-phase region does not seem to affect these peaks although they

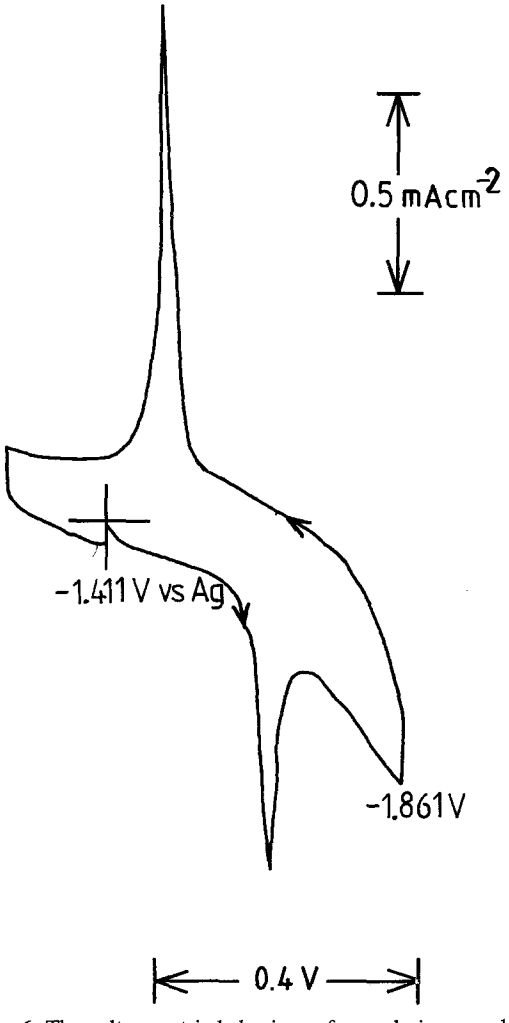

Fig. 6. The voltammetric behaviour of a newly-immersed aluminium electrode. Sweep rate: 100 mVs^{-1}. This figure was originally presented at the Fall 1980 meeting of the Electrochemical Society, Inc. held in Hollywood, Florida, USA.

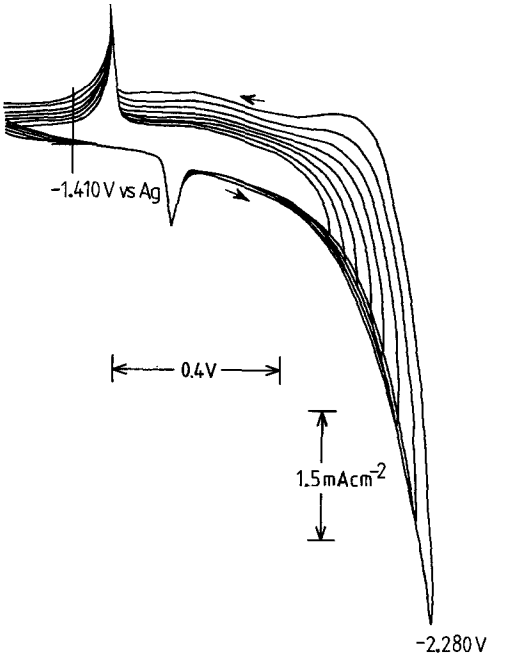

Fig. 7. The effects of lithium deposition and dissolution on the behaviour of a newly-immersed aluminium electrode. Sweep rate: 100 mVs^{-1}. This figure was originally presented at the Fall 1980 meeting of the Electrochemical Society, Inc. held in Hollywood, Florida, USA.

do disappear after the electrode is exposed to repeated cycling of the β-phase. There is, of course, the possibility that these peaks may be due to electrode processes involving hydroxides and oxides of aluminium. In this regard it is perhaps worth noting that OH^- ions are cathodically electroactive on platinum at + 0.47 Vs the Li–Al reference electrode [26].

Two more pre-peaks, which only appear with newly-immersed aluminium electrodes, are revealed (Fig. 8) if switching is carried out at more cathodic potentials in the β-phase formation region. These occur at + 20 and + 100 mv respectively, vs the Li/Al reference electrode and are very sharp. The charge under one of them is about 75 μC cm^{-2}. They gradually disappear with cycling in the β-phase region or after the aluminium electrode is immersed in the melt for a few hours. It is tempting to speculate that they are due to the predeposition of lithium atoms (to form the β-phase with the underlying aluminium) on energetically favourable sites and that these sites are annealed out during either operation or prolonged immersion on open-circuit.

3.6. *Scanning coulometry*

The phenomena taking place on the aluminium substrate following the predeposition of lithium are further exemplified by the results of scanning coulometry experiments shown in Figs 9 and 10. Figure 9 is a plot of total charge vs electrode potential, whereas Fig. 10 shows the same data but this time plotted as the average charge to take account of the variation of time elapsed during a sweep when different switching potentials are

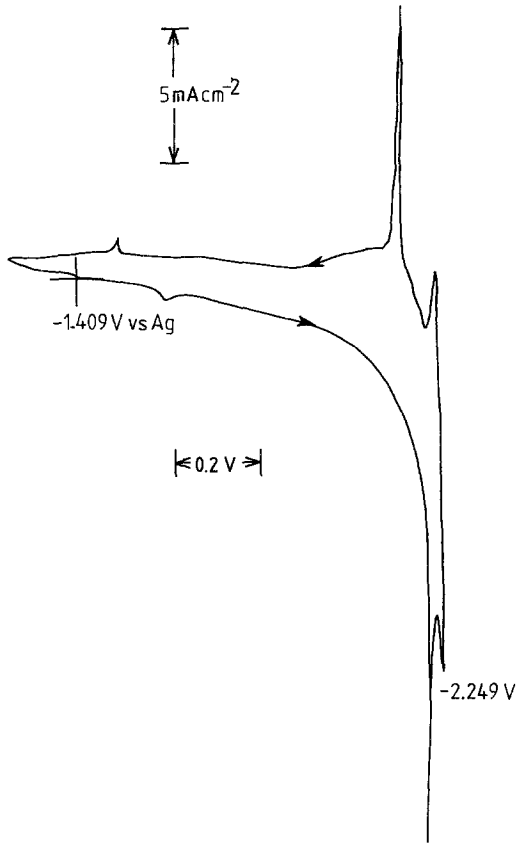

Fig. 8. The behaviour of a newly-immersed aluminium electrode in the β-phase formation region. Sweep rate: 100 mVs^{-1}. This figure was originally presented at the Fall 1980 meeting of the Electochemical Society, Inc. held in Hollywood, Florida, USA.

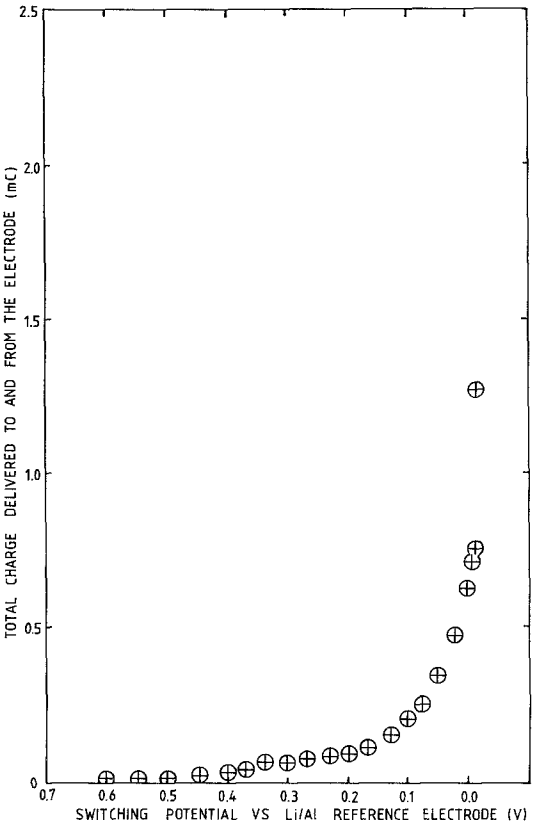

Fig. 9. Switching potential versus total charge delivered to the aluminium electrode. This figure was originally presented at the Fall 1980 meeting of the Electrochemical Society, Inc. held in Hollywood, Florida, USA.

utilised. Undervoltage deposition is clearly exemplified as well as the absence of a well defined threshold potential for the formation of the solid solution (α-phase) and the very marked increase of charge passed during the formation of the β-phase.

The extents of the anodic and the cathodic charges are shown in Figs 11 and 12. In the α-phase formation region, the anodic charge is always less than the cathodic charge at the same switching potential. However, as the switching potential moves into the β-phase formation region the ratio moves closer to unity. The most obvious (and intrinsic) explanation for this reversibility of the charging process is that in this phase the lithium atoms are present in easily accessible sites. An alternative explanation is that the effects of impurities are less marked as the charging and discharging currents increase. This is also illustrated by the fact that the coulombic efficiency is increased with increasing sweep rate (Table 1) at a potential just below the formation of the β phase.

3.7. *Dependence of the formation potential of the β-phase on the sweep rate*

Fig. 13 shows clearly that the slower the sweep rate, the sharper is the β-phase formation peak because the behaviour corresponds more closely to that at equilibrium. At the slowest sweep rate it is noteworthy that the cathodic and anodic peaks are identical. However, the most important factor which emerges from the variation of sweep rate is that the formation potential for the β-phase shifts in the cathodic direction with increase of

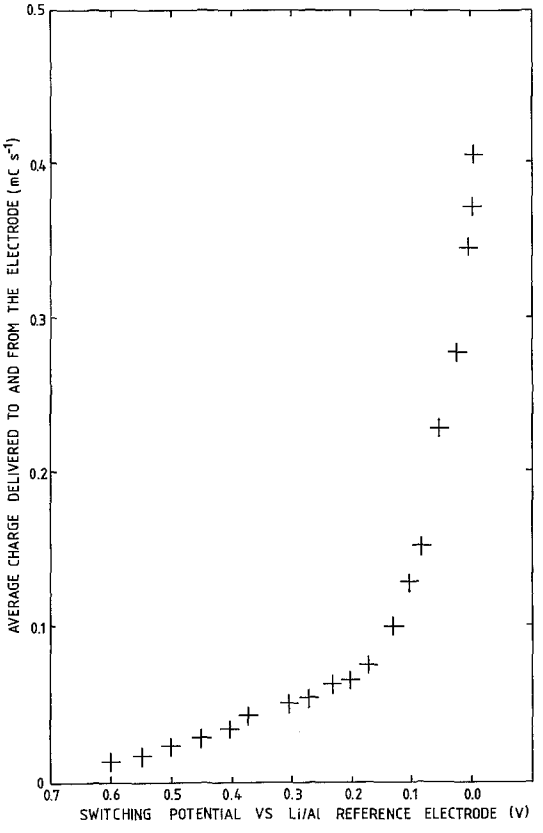

Fig. 10. Switching potential versus average charge delivered to the aluminium electrode. This figure was originally presented at the Fall 1980 meeting of the Electrochemical Society, Inc. held in Hollywood, Florida, USA.

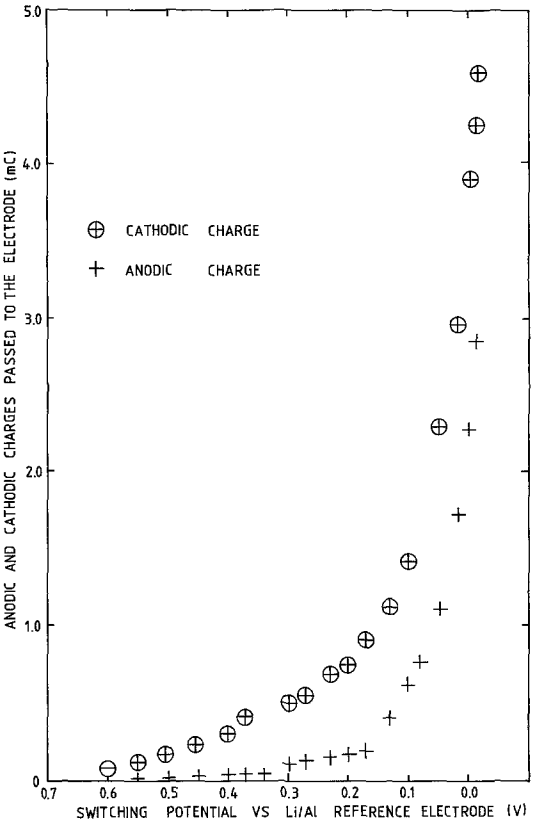

Fig. 11. Switching potential versus anodic and cathodic charges delivered to the aluminium electrode. This figure was originally presented at the Fall 1980 meeting of the Electrochemical Society, Inc. held in Hollywood, Florida, USA.

sweep rate. (In the present study, it is seen that the switching potential has to be shifted in the negative direction in order to observe the β-phase formation peak with increasing sweep rate.) On these grounds it is reasonable to speculate that this behaviour results from nucleation polarization to germinate the β-phase. Thus, a more negative potential as well as a longer time at the β phase formation potential will be allowed for the formation of appreciable β phase at the electrode surface leading subsequently to the appearance of the stripping peak.

3.8. *The effects of more cathodic switching*

The effects of sweep rate when the switching potential is made even more negative (> 0.2 V negative to the β-phase potential) are shown in Fig. 14. Switching is now being carried out after the appearance of a conventional linear sweep voltammetric maximum. This indicates that the current is limited by the rate of diffusion of lithium through the β-phase. The most noteworthy feature is that, for post-peak switching at the same electrode potential, the current during the

Table 1. Effect of scan rate on cyclic efficiency E_R = + 0.8 V versus Li/Al reference electrode. Switching potential = 0.0 V just before formation of stripping peak

Sweep rate (mVs^{-1})	*Cyclic efficiency*
20	0.09026
50	0.1842
75	0.2649
150	0.3664
300	0.3893

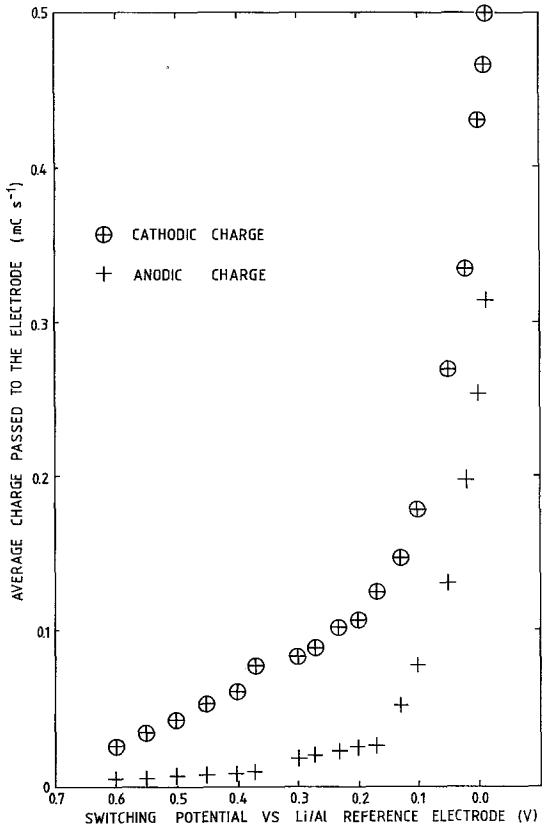

Fig. 12. Switching potential versus average anodic and cathodic charges delivered to the aluminium electrode. This figure was originally presented at the Fall 1980 meeting of the Electrochemical Society, Inc. held in Hollywood, Florida, USA.

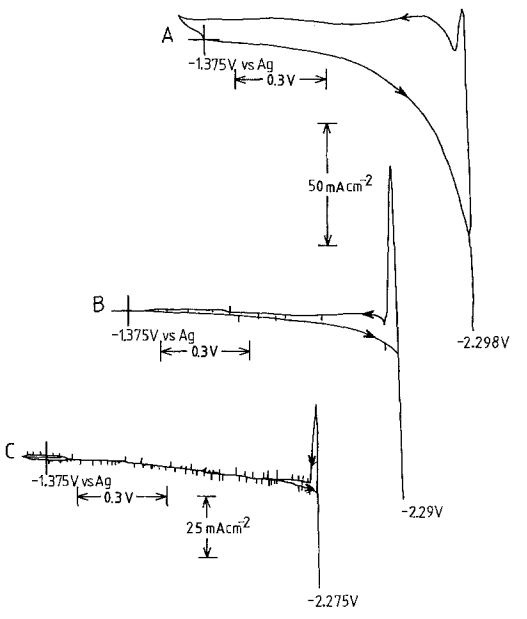

Fig. 13. The effect of the sweep rate on the formation of the β-phase. Sweep rate (m Vs^{-1}): A, 100; B, 10; C, 1. This figure was originally presented at the Fall 1980 meeting of the Electrochemical Society, Inc. held in Hollywood, Florida, USA.

reverse sweep is smaller than during the forward sweep. The steepness of the slopes of the deposition and stripping waves indicates that the electrode is well poised and that the current is limited mainly by the uncompensated resistance of the cell. Current oscillations appear at low sweep rates, presumably as a result of changes in the (active) surface area of the electrode due to the extensive alloying between lithium and the aluminium electrode.

3.9. *Effects of holding the electrode potential in the β-phase formation region*

It can be seen (Fig. 15) that two stripping (anodic) peaks manifest themselves following the 'hold' whereas, if the reverse sweep is carried out immediately following the forward (cathodic) sweep, only one stripping peak appears. The height of the second (more anodic) peak increases with 'hold' time whereas the height of the first peak only increases slightly.

It is probable that this phenomenon arises because the lithium atoms have time (with increasing 'hold' time) to diffuse from their initial sites to more (energetically) stable sites. Needless to say an extrinsic explanation based on impurity effects could also be invoked here.

3.10. *Switching at extreme cathodic potentials*

Fig. 16 shows that two pairs (anodic/cathodic) of peaks appear in this region. The potentials indicate that the larger pair probably results from the formation (cathodic) and dissolution (anodic) of liquid alloy and that the smaller pair results from the formation and dissolution of the γ-phase. The electrode potentials for both sets however are slightly more negative than their equilibrium potentials which perhaps indicates that their formation is attended by nucleation polarization. Large currents are finally manifested at the most

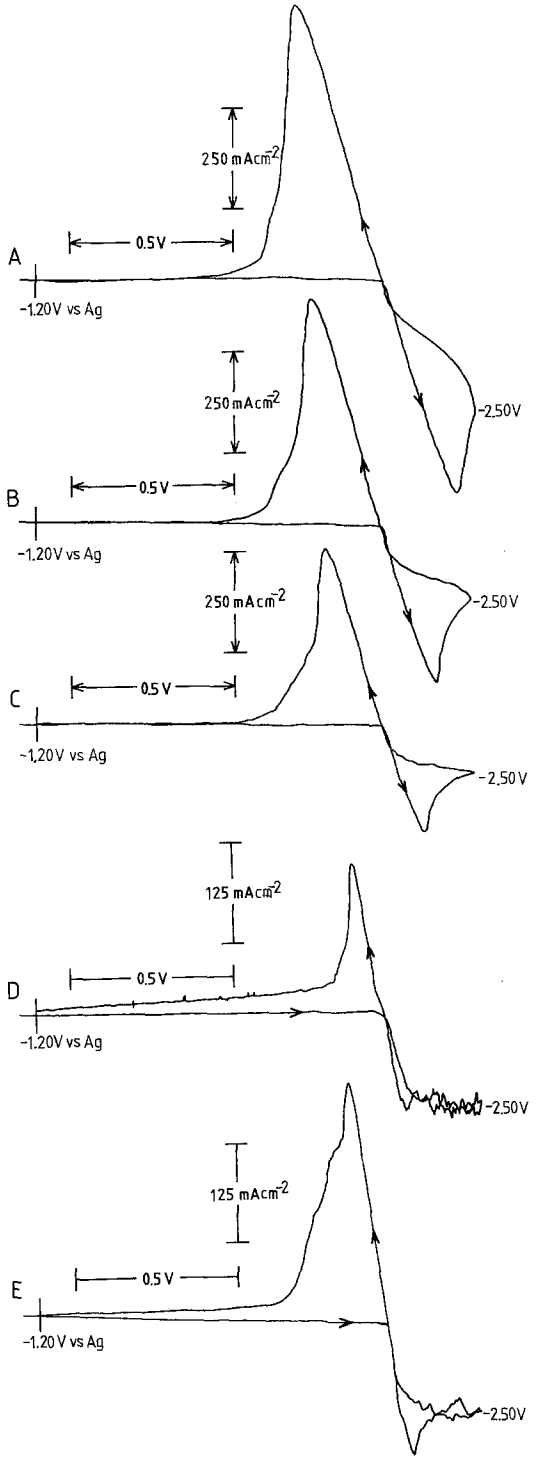

Fig. 14. The effect of scan rate on the deposition of lithium on aluminium. Sweep rate (m Vs^{-1}): A, 100; B, 50; C, 20; D, 2; E, 5. This figure was originally presented at the Fall 1980 meeting of the Electrochemical Society, Inc. held in Hollywood, Florida, USA.

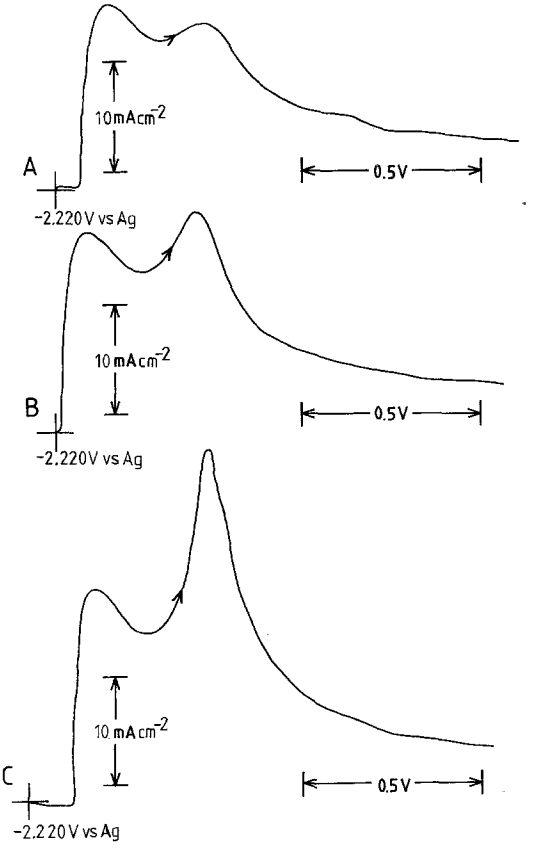

Fig. 15. The effect of different hold times on the stripping voltammogram. Hold time: A, 5 mins; B, 15 mins; C, 55 mins. Hold potential: −2.220 V versus Ag/AgCl (0.2 mol%). Reverse sweep rate: 100 mVs^{-1}. This figure was originally presented at the Fall 1980 meeting of the Electrochemical Society, Inc. held in Hollywood, Florida, USA.

negative potentials, the cathodic limit (Fig. 16C and D). The appearance of current oscillations in the region of the anodic peaks is accompanied by the evolution of gases from the electrode surface and the disappearance of the peaks due to lithium dissolution. Thus the formation of potassium (which is a vapor at 400° C) by the displacement reaction

$$Li + KCl \rightarrow K + LiCl$$

is likely to take place, even though the equilibrium state would be expected to lie to the left, because the reaction is driven by the loss of potassium from the system. To confirm this hypothesis, lithium metal was added to the melt and a voltammogram recorded. The melt turned a reddish-

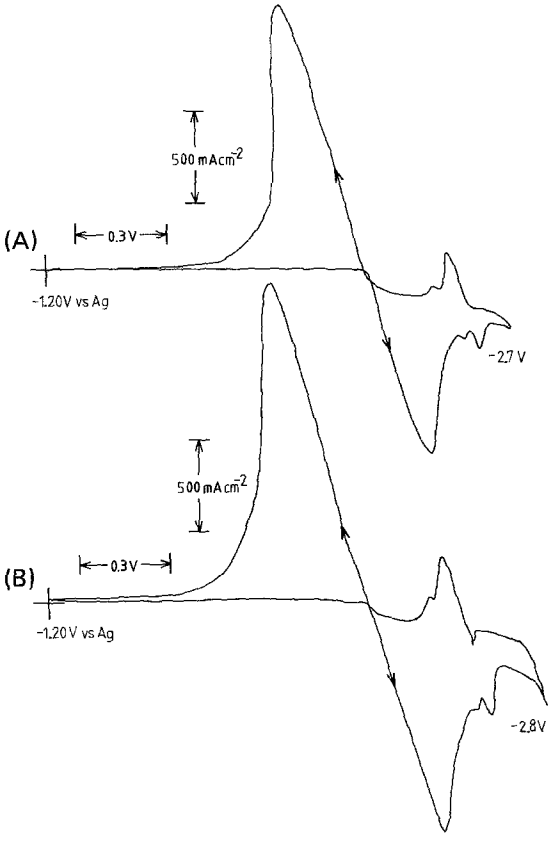

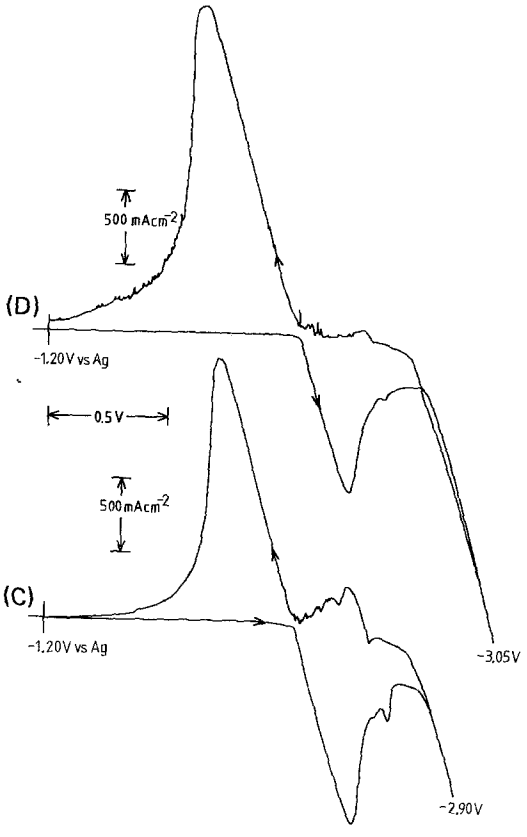

Fig. 16. The effect of switching potential on the deposition of γ-phase and liquid lithium-aluminium alloy. Switching potential: A, — 2.70 V; B, — 2.80 V; C, — 2.90 V; D, — 3.05 V; versus Ag/AgCl (0.2 mol %). Rest potential: — 1.2 V versus Ag/AgCl reference electrode (0.2 mol %). Sweep rate: 100 mV s^{-1}. This figure was originally presented at the Fall 1980 meeting of the Electrochemical Society, Inc. held in Hollywood, Florida, USA.

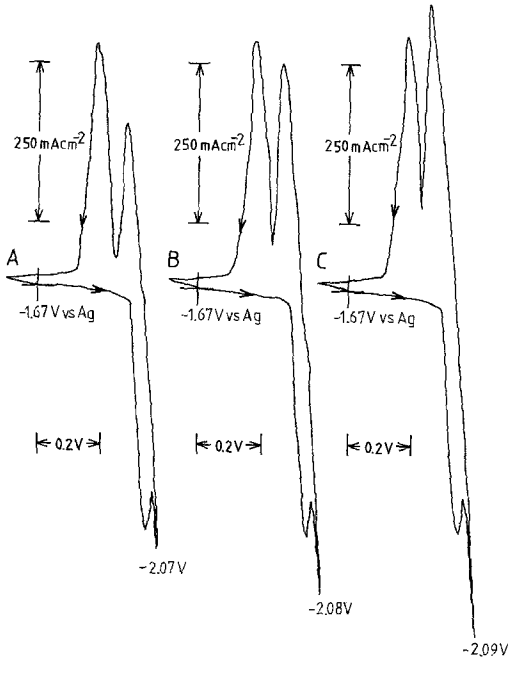

Fig. 17. The effect of the switching potential on the stripping of lithium and potassium in the presence of dissolved lithium metal. Sweep rate: 100 mV s^{-1}. This figure was originally presented at the Fall 1980 meeting of the Electrochemical Society, Inc. held in Hollywood, Florida, USA.

brown and a red deposit appeared on the cool surfaces above the melt. Fig. 17 shows that a stripping peak for potassium then appeared.

4. Conclusions

It may be concluded that:

1. Undervoltage deposition of lithium on aluminium takes place mainly by the formation of a solid solution (the α-phase) and the β-phase.

2. There is no clear cut threshold potential for the formation of the α-phase.

3. There is a critical potential for the formation of the β-phase which seems to be accompanied by a nucleation polarization.

4. Once the β-phase is formed, the electrode is well poised (as evidenced by the linear sweep voltammograms) and can sustain a high current with minimum polarization.

5. The phenomena occurring at the electrode and their kinetics are very much influenced by the surface states of the electrode. Deposited metal monolayers may be involved but oxide/hydroxide arising from impurities can also play a part.

6. Fast cycling of the electrodes leads to their "development" i.e., both the anodic and cathodic currents increase.

7. If the potential is made too negative potassium can form. This would have a deleterious effect by leading to electronic conduction.

Acknowledgements

We thank the Ministry of Defence for its support of this work and Mr. L. Pearce of the Admiralty Marine Technology Establishment for helpful discussions.

References

[1] E. G. Gay, D. R. Vissers, F. J. Martino and K. E. Anderson, *J. Electrochem. Soc.* **123** (1976) 1591.
[2] W. J. Walsh and H. Shimotake, *Proc. 10th Internat. Power Sources*, (edited by D. H. Collins) Academic Press, London, (1977) p. 725.
[3] J. R. Selman, D. K. DeNuccio, C. J. Sy and R. K. Steunenberg, *J. Electrochem. Soc.* **124** (1977) 1160.
[4] C. J. Wen, W. Weppner, B. A. Boukamp and R. A. Huggins, *ibid.* **126** (1979) 2258.
[5] C. A. Melendres, *ibid.* **124** (1977) 650.
[6] A. L. L'vov and A. A. Gnilomedov, *Sov. Electrochem.* **11** (1975) 473.
[7] S. D. James, *Electrochim. Acta* **21** (1976) 157.
[8] J. E. B. Randles, *Trans. Faraday Soc.* **44** (1948) 322.
[9] R. S. Nicholson, *Anal. Chem.* **37** (1965) 667.
[10] *Idem, ibid.* **37** (1965) 1351.
[11] R. S. Nicholson and I. Shain, *Anal. Chem.* **37** (1965) 190.
[12] R. S. Nicholson, *Anal. Chem.* **38** (1966) 1406.
[13] R. C. Propst, *J. Electroanal. Chem. Interfac. Electrochem.* **16** (1968) 319.
[14] *Idem, Anal. Chem.* **35** (1963) 958.
[15] *Idem, ibid.* **41** (1969) 910.
[16] F. Ying-Sing, PhD thesis, London University (1980).
[17] D. G. Lovering, (ed), 'Molten Salts Techniques', Plenum, (New York) to be published.
[18] R. P. Elliott, 'Constitution of Binary Alloys', first supplement, McGraw-Hill Ltd., New York , (1965) p. 42.
[19] M. Hansen, 'Constitution of Binary Alloys', McGraw-Hill Ltd., New York, (1958) pp. 104–5.
[20] F. A. Shunk, 'Constitution of Binary Alloys', second supplement, McGraw-Hill Ltd., New York, (1969) pp. 27–8.
[21] S. D. James, *Electrochim. Acta* **21** (1976) 157.
[22] L. P. Costas, US At. Energy Commn. Report, TID-16676, (1963) 7pp.
[23] L. P. Costas and R. P. Marshall, *Trans. AIME* **224** (1962) 970.
[24] G. J. Hills, D. J. Schiffrin and J. Thompson, *J. Electrochem. Soc.* **120** (1973) 157.
[25] M. M. Nicholson, *J. Amer. Chem. Soc.* **79** (1957) 7.
[26] C. A. Melendres, J. P. Ackerman and R. K. Steunenberg, *Proc. Internat. Symp. on Molten Salts* Electrochem. Soc. (1976) p. 575.